BJR

Received: 30 September 2015 | Revised: 12 September 2016 | Accepted: 19 September 2016

http://dx.doi.org/10.1259/bjr.20150806

Cite this article as:
Jeon TY, Kim JH, Im GH, Kim J-H, Yang J, Yoo S-Y, et al. Hollow manganese oxide nanoparticle-enhanced MRI of hypoxic-ischaemic brain injury in the neonatal rat. *Br J Radiol* 2016; **89**: 20150806.

FULL PAPER

Hollow manganese oxide nanoparticle-enhanced MRI of hypoxic-ischaemic brain injury in the neonatal rat

[1]TAE YEON JEON, MD, [1]JI HYE KIM, MD, [2]GEUN HO IM, PhD, [2]JAE-HUN KIM, PhD, [2]JEHOON YANG, PhD, [1]SO-YOUNG YOO, MD and [2]JUNG HEE LEE, PhD

[1]Department of Radiology and Center for Imaging Science, Samsung Medical Center, Sungkyunkwan University School of Medicine, Seoul, Republic of Korea
[2]Department of Radiology and Center for Molecular and Cellular Imaging, Samsung Medical Center, Sungkyunkwan University School of Medicine, Seoul, Republic of Korea

Address correspondence to: Prof. Ji Hye Kim
E-mail: *jhkate@skku.edu*

Objective: To determine the utility of hollow manganese oxide nanoparticle (HMON)-enhanced MRI in depicting and monitoring apoptotic area following hypoxic–ischaemic injury in a neonatal rat brain and to evaluate the longitudinal evolution of hypoxic–ischaemic brain injury (HII) up to 21 days.
Methods: The institutional animal care and use committee approval was obtained. The Rice–Vannucci model of HII was used in 7-day-old rat pups ($n = 17$). MRI was performed 1, 3, 7, 14 and 21 days after HII with intraperitoneal injection of HMON. Relative contrast values in the injured hemisphere and mean apparent diffusion coefficient values were calculated at each time point. Apoptosis and reactive astrogliosis were detected by terminal deoxynucleotidyl transferase-mediated dUTP-biotin nick end-labelling (TUNEL) and glial fibrillary acidic protein staining, and the distribution and intensity of immunohistochemical staining were directly compared with those of HMON enhancement on MRI.
Results: The dorsolateral thalamus, hippocampus and remaining cortex of the injured hemisphere showed HMON enhancement from 3 to 21 days after HII. The mean relative contrast values in the dorsolateral thalamus showed an increase from a negative value at 1 day to $16.5 \pm 4.8\%$ at 21 days. The apoptotic cells and reactive astrocytes were observed on immunohistochemical staining from 1 to 21 days after HII. The accumulation of apoptotic cells regionally matched with the areas of HMON enhancement, while that of reactive astrocytes did not.
Conclusion: The areas of HMON enhancement showed best spatial agreement with those of apoptosis on TUNEL staining. Both HMON enhancement and TUNEL-positive cells were observed up to 21 days after HII.
Advances in knowledge: The strength of our study is the visualization of apoptotic area *in vivo* using HMON-enhanced MRI, and we also showed that HII has a prolonged evolution lasting for several weeks.

INTRODUCTION

Perinatal hypoxic–ischaemic brain injury (HII) is a major cause of mortality and morbidity in infants and young children.[1,2] In contrast to the immediate irreversible damage caused by infarction, HII leads to a prolonged neuronal death after the insult. Apoptosis contributes significantly to the delayed death of neurons following the insult.[3,4] It may be possible to block the neurochemical cascade that initiates the delayed injury process. Multiple therapeutic trials are currently being conducted to investigate effective antiapoptotic therapy against HII.[5–8] Therefore, the availability of a technique to image apoptotic cell death *in vivo* is of considerable interest.

MRI can play an essential role in the assessment of HII, providing the opportunity to perform longitudinal imaging of the injury process *in vivo*.[9,10] Apparent diffusion coefficient (ADC) values may be useful for assessing early phase of HII, but their use may be limited in identifying subsequent processes because pseudonormalization of the ADC values can occur.[11,12] Manganese-enhanced MRI has been used in animal models, since it enables the visualization of neuroarchitecture.[10,13–15] Clinical application of manganese-enhanced MRI, however, is limited by safety issues concerning the toxicity of high-dose manganese.[16,17]

Therefore, it is highly desirable to explore a novel MR method, which is capable of depicting apoptotic cell death after HII. Hollow manganese oxide nanoparticle (HMON) was recently developed as a positive T_1 contrast agent for MRI. HMON has an enhanced relaxivity attributed to its large water-accessible surface area, improved diagnostic

performance with long blood circulation time and the flexibility of many options for functional modifications of the surface and hollow centre.[18,19]

The aim of our study was to determine the utility of HMON-enhanced MRI in depicting and monitoring apoptotic area following hypoxic–ischaemic injury in a neonatal rat brain and to evaluate the longitudinal evolution of HII up to 21 days.

METHODS AND MATERIALS

All of the experimental protocols were approved by the Institutional Animal Care and Use Committee of the Samsung Biomedical Research Institute. The Samsung Biomedical Research Institute is an Association for Assessment and Accreditation of Laboratory Animal Care International-accredited facility and abides by the Institute of Laboratory Animal Resources guide.

Animal model of hypoxic–ischaemic brain injury

HII was induced using the Rice–Vannucci model[20,21] in 7-day-old Sprague–Dawley rat pups ($n = 17$, 13–17 g). The right common carotid artery was exposed and ligated under isoflurane anaesthesia (4% for induction and 2% for maintenance). The duration of operating procedure was <5 min. The pups were then allowed to recover with their dam for at least 2 h. Hypoxia was induced by placing the pups in a fibreglass cage containing humidified gas mixture (8% O_2-balance N_2) for 180 min and maintained at around 36 °C throughout the procedure. This procedure resulted in unilateral HII to the right cerebral hemisphere.

MR image acquisition

MRI was performed on 1, 3, 7, 14 and 21 days after HII using a 7.0-T MRI system (Bruker Biospin, Fallanden, Switzerland) equipped with a 20-cm gradient set capable of supplying up to 400 mT m^{-1} with a rise time of 100 μs. A birdcage coil (inside diameter, 72 mm; Bruker Biospin, Fallanden, Switzerland) was used for excitation, and an actively decoupled phased-array coil was used for signal reception. During scanning, the anaesthetized (isoflurane, 4% for induction and 1–1.5% for maintenance) pups lay prone in a dedicated water-heated bed and the head of the pup was carefully fixed using earplugs, a tooth bar and a nose mask. Temperature and respiration were monitored during scanning. HMON was given as a dose of 20 mg kg^{-1} body weight at a concentration of 100 mM (mixed with 0.9% NaCl to a volume of 0.1 ml) by intraperitoneal injection to all of the pups just before inducing HII.

All MR images were scanned with a total of 12 slices and a 1.0-mm slice thickness without interslice gaps that encompassed the entire brain for an average of 26 min per pup. Coronal scans were obtained using the following sequences: fast spin-echo T_1 weighted images [repetition time (TR)/echo time (TE) = 232/7.7 ms, number of experiments (NEX) = 12, field of view (FOV) = 25.6 × 25.6 mm^2, matrix = 256 × 256, duration = 12 min] and fast spin-echo T_2 weighted images (TR/TE = 3000/60 ms, NEX = 2, FOV = 25.6 × 25.6 mm^2, matrix = 256 × 256, duration = 6.5 min). Diffusion-weighted images were obtained using an echoplanar imaging sequence (TR/TE = 3000/100 ms, b-values = 0/100/200/400/600/800/1000 s mm^{-2}, NEX = 5, FOV = 25.6 × 25.6 mm^2, matrix = 128 × 128, repetitions = 3, duration = 7 min). ADC values were computed in a voxel-by-voxel manner using in-house-developed software (MATLAB® v. R2008a; MathWorks Inc., Natick, MA) by exponential fitting of the local signal intensity *vs* b-values.

Three pups without lesions on MRI were presumed to have no hypoxic–ischaemic lesions and were excluded from the study. Thus, a total of 14 pups were included in this study.

Histology and immunohistochemistry

After MRI acquisition, animals were sacrificed at 1 day ($n = 2$), 3 days ($n = 2$), 7 days ($n = 2$), 14 days ($n = 2$) and 21 days ($n = 6$) following HII. They were anaesthetized with 1.5% isoflurane and were perfused intracardially with 0.9% normal saline followed by 4% paraformaldehyde in phosphate-buffered saline. Brains were removed and serially sliced into coronal sections (4-μm thick) using a brain matrix along the same plane as MRI sections. Slides were processed for standard staining with haematoxylin–eosin (H&E) and immunohistochemical staining with terminal deoxynucleotidyl transferase-mediated dUTP-biotin nick end-labelling (TUNEL) as a marker for apoptosis and antiglial fibrillary acidic protein as a marker for reactive astrocytes.

Data analysis

Two radiologists (with 20 and 5 years' paediatric imaging interpretation experiences, respectively), who were blinded to the histological results, evaluated all of the MR images by consensus. The sequential changes in the hypoxic–ischaemic brain were evaluated at five time points, with emphasis on the presence of enhancement in the injured hemisphere on T_1 weighted images and the signal intensity in the injured hemisphere on T_2 weighted and diffusion-weighted images.

For quantitative measurement of contrast enhancement in the injured hemisphere on T_1 weighted images and the signal intensity in the injured hemisphere on T_2 weighted images, the relative contrast values were calculated using the following equation:

$$\text{Relative contrast value} = \left[\text{signal intensity}_{\text{ROI(ipsilateral)}} - \text{signal intensity}_{\text{ROI(contralateral)}}\right] \Big/ \text{signal intensity}_{\text{ROI(contralateral)}} \times 100.$$

The circular regions of interest (ROIs) (area, 0.16 mm^2) were manually drawn in the dorsolateral thalamus at the level of the hippocampal head on T_1 and T_2 weighted images. Lesions were mirrored to the contralateral brain as reference ROIs. All data are expressed as mean ± standard deviation. In addition, ROI analysis of the mean ADC value in the dorsolateral thalamus was performed and mirroring of ROIs in the contralateral hemisphere was also performed for comparison.

The slices stained for immunohistochemistry were evaluated using standard microscopy. For assessing the colocalization between histopathologic findings and MR images, the distribution of TUNEL-stained and glial fibrillary acidic protein (GFAP)-stained cells in different areas of the injured hemisphere was visually compared with that of HMON enhancement at the level of the hippocampal head. For comparison between histopathologic images and MR images, the stained histopathologic images were converted into greyscale images and then, the grey levels of these images were manually adjusted to be comparable with the HMON-enhanced MR images using in-house-developed software (MATLAB® v. R2008a; MathWorks Inc.). We evaluated the morphological changes in the injured hemisphere and the presence of haemorrhage on H&E staining.

RESULTS

Contrast-enhanced T_1 and T_2 weighted images

Contrast-enhanced T_1 weighted images of the injured hemisphere showed enhancement in a part of the dorsolateral thalamus, hippocampus and remaining cortex from 3 to 21 days after HII. Most of the cortex and hippocampus in the injured hemisphere were liquefied during the period from 7 to 21 days, appearing as hypointense areas on contrast-enhanced T_1 weighted images. HMON enhancement was also seen along the edge of the remaining cortex and hippocampus (Figure 1). Chronological changes in the relative contrast values in the injured hemisphere on T_1 and T_2 weighted images are shown in Figure 2. The dorsolateral thalamus in the injured hemisphere showed signal reduction compared with that of contralateral hemisphere, representing negative relative contrast values at 1 day. The mean relative contrast values in the dorsolateral thalamus on T_1 weighted images were notably increased to $5.7 \pm 3.7\%$ at 3 days after HII and then gradually increased to $16.5 \pm 4.8\%$ up to 21 days.

Contrast-enhanced T_2 weighted images demonstrated transient hyperintensity at 1 day, but thereafter they showed persistent hypointensity till 21 days. The areas of T_2 hypointensity clearly corresponded to those of T_1 hyperintensity. The mean relative contrast values in the injured hemisphere decreased from $-19.3 \pm 10.9\%$ to $-49.6 \pm 12.2\%$ during the period from 3 to 21 days.

Figure 1. Serial brain MR images in a pup after hypoxic–ischaemic brain injury: (a) contrast-enhanced T_1 weighted images (T1WI) are showing hollow manganese oxide nanoparticle enhancement in a part of the dorsolateral thalamus, hippocampus and cortex of the injured hemisphere from 3 to 21 days. Large areas of the cortex in the injured hemisphere are showing cavitary changes from 7 to 21 days. (b) Contrast-enhanced T_2 weighted images (T2WI) are showing hyperintensity in the injured hemisphere at 1 day and hypointensity in a part of the dorsolateral thalamus, hippocampus and cortex of the injured hemisphere up to 21 days. The areas of T_2 hypointensity are clearly corresponding to those of T_1 hyperintensity (asterisks at the dorsolateral thalamus). (c, d) An injured hemisphere is showing hyperintensity on diffusion-weighted images and decreased apparent diffusion coefficient (ADC) values at 1 day. From 3 to 21 days, there is an increase in ADC values of the injured hemisphere. DWI, diffusion-weighted imaging.

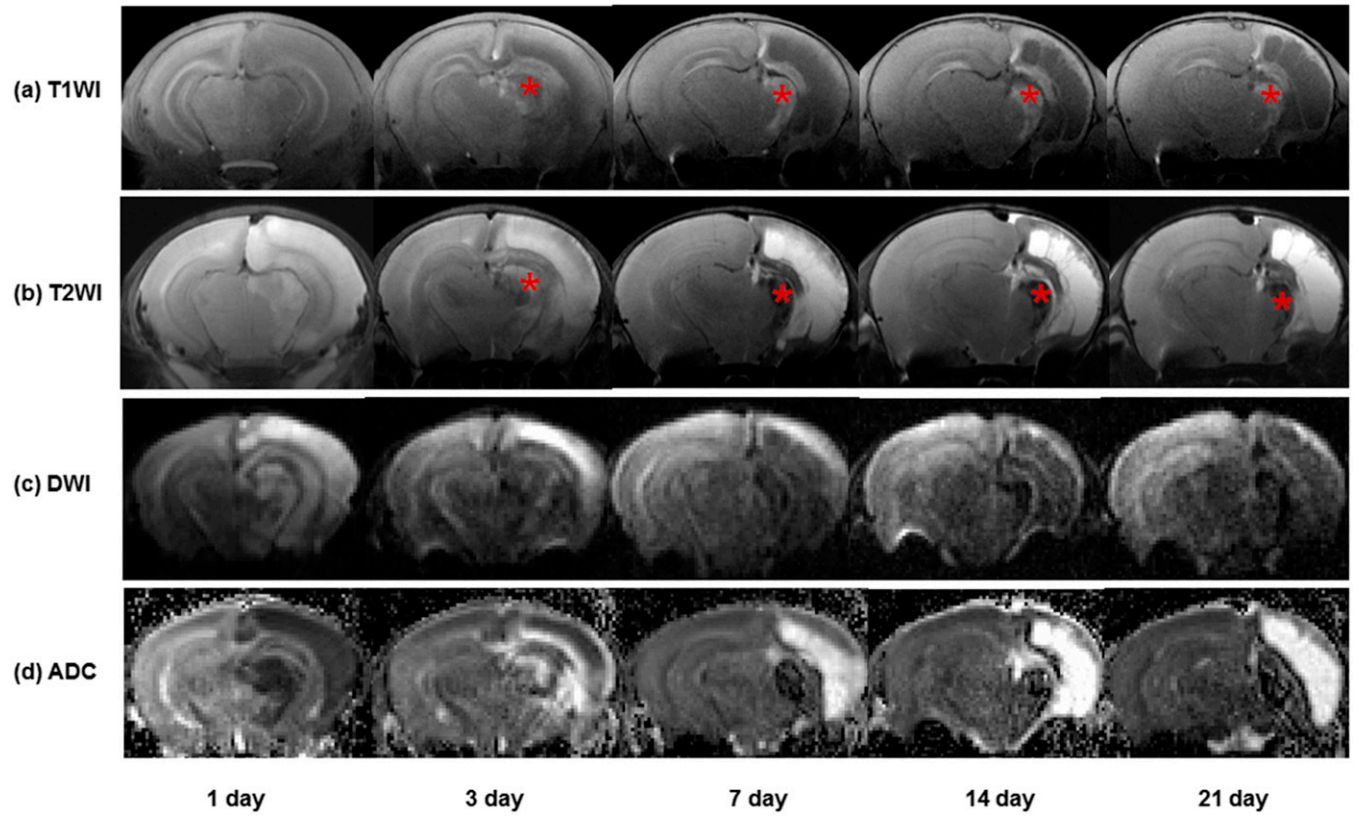

Figure 2. Mean relative contrast values in the dorsolateral thalamus at each time point are showing an increase from a negative value at 1 day to 16.5 ± 4.8% at 21 days on T_1 weighted images (T1WI) and a decrease from a positive value at 1 day to −49.6 ± 12.2% at 21 days on T_2 weighted images (T2WI).

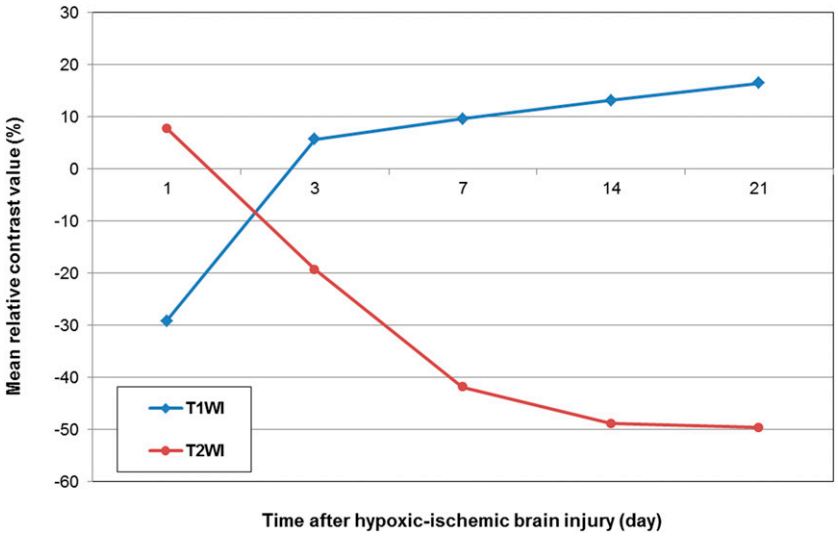

Diffusion-weighted images and apparent diffusion coefficient maps

At 1 day after HII in all of the pups, the injured hemisphere showed hyperintense areas on diffusion-weighted images and a corresponding decrease in ADC compared with the contralateral hemisphere. From 3 to 21 days, the ADC values in the dorsolateral thalamus and remaining cortex of the injured hemisphere were gradually increased, while those of the contralateral hemisphere were decreased. There was a signal loss in the dorsolateral thalamus of the injured hemisphere, which corresponded to hypointensity on T_2 weighted images (Figure 1). The changes in the mean ADC values of the dorsolateral thalamus following HII are shown in Figure 3. Mean ADCs in the dorsolateral thalamus of the injured hemisphere at 1 day and 3 days were lower by 0.436×10^{-3} and 0.745×10^{-3} $mm^2 s^{-1}$, respectively, than those of the contralateral hemisphere ($p < 0.001$ and $p = 0.002$). Mean ADC in the dorsolateral thalamus of the injured hemisphere returned to normal at 7 days.

Figure 3. Mean apparent diffusion coefficient (ADC) values in the dorsolateral thalamus at each time point are showing decreased mean ADC values in the dorsolateral thalamus of the injured hemisphere compared with those of the contralateral hemisphere from 1 day to 3 days. Mean ADC values in the dorsolateral thalamus of the injured hemisphere are normalized at 7 days. Asterisks are indicating significant differences ($p < 0.05$, two-sample t-test) in mean ADC values between the dorsolateral thalamus of the injured and contralateral hemispheres. Injured = dorsolateral thalamus of the injured hemisphere; contralateral = dorsolateral thalamus of the contralateral hemisphere.

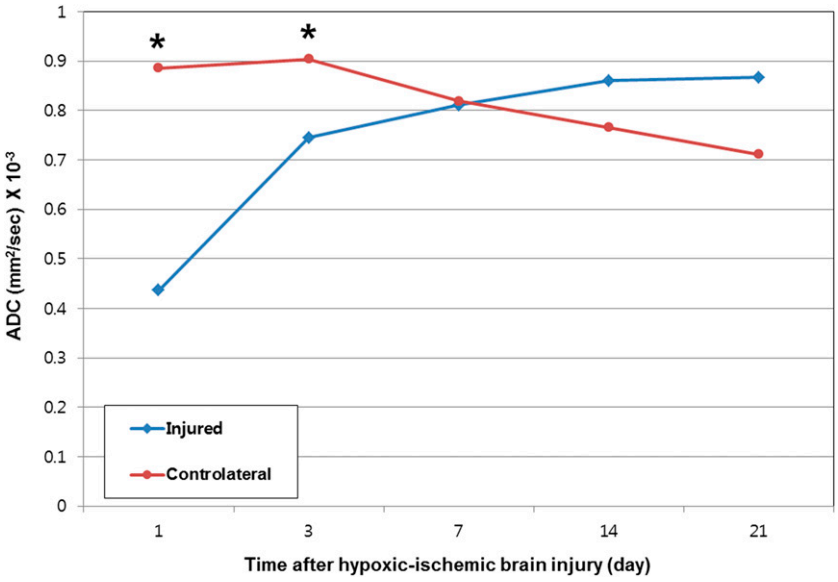

Colocalization of histological findings and MRI

All of the pups revealed histopathological changes in the injured hemisphere on TUNEL, GFAP and H&E staining.

Immunohistochemical examination of brain sections showed high number of TUNEL-positive cells in the dorsolateral thalamus, hippocampus and cortex of the injured hemisphere. TUNEL-positive cells in the injured hemisphere were observed from 1 day, peaked at 3 days and then declined till 21 days after HII (Figure 4). Areas of TUNEL-positive cells were regionally limited and matched obviously with those showing HMON enhancement on T_1 weighted MR images from 3 to 21 days. Although TUNEL-positive cells were widely spread in the large parts of the thalamus, hippocampus and cortex of the injured hemisphere, there was no HMON enhancement at 1 day in all of the pups (Figure 5).

On the contrary, HMON enhancement did not show spatial agreement with the distribution of the GFAP immunoactivity, although the distribution of the GFAP-positive cells did partially overlap with the HMON enhancement. GFAP-positive regions indicating the presence of reactive astroglia were seen throughout the entire injured hemisphere. The positive areas of GFAP staining were larger than those of TUNEL staining. There was a tendency for a negative correlation between the positive areas of TUNEL staining and those of GFAP staining. There was a weaker staining for GFAP in the injured hemisphere with accompanying high number of TUNEL-positive cells (Figure 5). GFAP-positive cells were observed at 1 day and they showed a persistent increase in number over time up to 21 days (Figure 4).

H&E stain revealed widespread tissue loss and formation of a large cyst in most of the cortex and spongiform appearance or formation of small cysts in the dorsolateral thalamus and hippocampus from 7 to 21 days. However, there was no haemorrhage in the injured hemisphere up to 21 days (data not shown).

Figure 4. Selected pixel numbers of immunohistochemical staining with terminal deoxynucleotidyl transferase-mediated dUTP-biotin nick end-labelling (TUNEL) and glial fibrillary acidic protein (GFAP) at each time point are showing that TUNEL-positive cells in the injured hemisphere are observed from 1 day, peak at 3 days and then decline by 21 days. Selected pixel numbers for GFAP-positive cells are showing an increase from 1 day to 21 days.

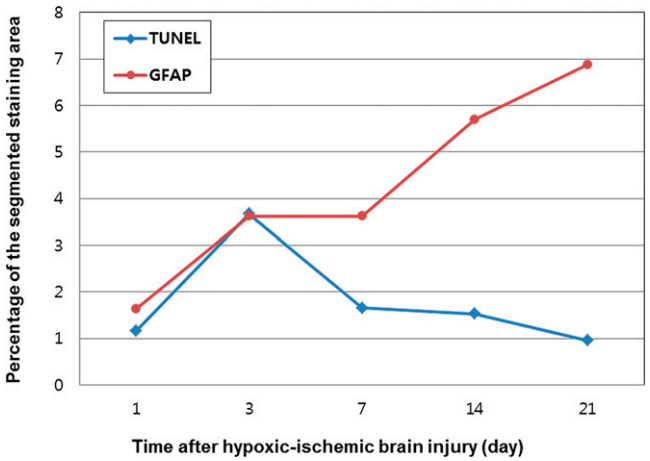

DISCUSSION

Our data demonstrated the feasibility of depicting apoptotic area after HII *in vivo* using MRI after intraperitoneal injection of HMON.

This study demonstrated the followings: (1) enhancement on HMON-enhanced T_1 weighted images as well as hypointensity on T_2 weighted images were seen in the dorsolateral thalamus, hippocampus and remaining cortex of the injured hemisphere in pups from 3 to 21 days after HII, (2) TUNEL-stained apoptotic cells and GFAP-stained reactive astrocytes in the injured hemisphere were observed up to 21 days after HII and (3) areas of HMON enhancement on T_1 weighted images showed best spatial agreement with those of apoptosis on TUNEL staining.

Apoptotic cascades are activated following neonatal HII in animal models. Recent data suggest, however, that apoptosis as a result of HII is morphologically different from developmental apoptosis, and many hybrid necrotic–apoptotic phenotypes have been observed.[3,22] Apoptosis is also referred to as delayed neuronal death because neurons do not die promptly but rather die within several hours to days after the insult. Immunohistochemical studies revealed that neonatal ischaemia-reperfusion model showed TUNEL-positive cells from 4 h to 30 days after reperfusion[23] and DNA fragmentation using ApopTag kit, which is known as an apoptotic marker, was initiated within 0.5 h and persisted for at least 4 weeks after HII.[24] In our study, an increase in the number of TUNEL-positive cells peaked at around 3 days after HII and maintained for 21 days. This implies that therapeutic efforts to block the enzymatic cascade of delayed neuronal death can be conducted up to 3 weeks following HII.

HMON, which was recently developed as a positive MR contrast agent, has proven its superiority in MRI contrast efficiency and drug-loading capacity. It has the ability to carry high payloads of MR-active magnetic centres owing to its large water-accessible surface area and it exhibits an improved diagnostic performance with long blood circulation time. In addition, it has the ability to load hydrophobic small molecules within the interior void, simultaneously with conjugation of the functional molecules at the surface area. HMON plays as dual contrast agent for T_1 and T_2 weighted MR images.[18,19] Although the mechanism for HMON accumulation remains unclear, it can be inferred that the increased relaxivity of the HMON is mainly due to the increased concentration of manganese ions exposed at the hollow inner surface.[18] We demonstrated HMON enhancement in the specific areas of the injured hemisphere after HII, which was in accordance with the results of previous studies using manganese-enhanced MRI.[9,15] HMON enhancement was seen at 3 days, which was earlier than that observed in the manganese-enhanced MR study by Widerøe et al.[15] Longitudinal manganese-enhanced MR studies showed delayed enhancement in the injured hemisphere up to 42 days, and it mainly corresponded to the areas of activated microglia and reactive astrocytes as well as low numbers of apoptotic cells.[9] Our results also

Figure 5. Colocalization of hollow manganese oxide nanoparticle (HMON)-enhanced MR images and immunohistochemical staining in five pups at each time point: (a) contrast-enhanced T_1 weighted images (T1WI) are showing no enhancement at 1 day. HMON enhancement is observed in a part of the injured hemisphere from 3 to 21 days. (b) Corresponding histologic slices with terminal deoxynucleotidyl transferase-mediated dUTP-biotin nick end-labelling (TUNEL) (original magnification, ×12.5) at 1 day are showing a weakly positive staining. TUNEL-positive cells in the injured hemisphere are increasing at 3 days and decreasing gradually by 21 days. (c) Corresponding slices with glial fibrillary acidic protein (GFAP) (×12.5) are showing increased areas of GFAP-positive cells from 1 day to 21 days. (d, e) Magnified slices of TUNEL (d) (red box) (×200) and GFAP (e) (blue box) (×200) are showing negative correlations between the positive areas of TUNEL staining and those of GFAP staining. The areas of TUNEL-positive cells (red asterisks) are negative or weakly positive for GFAP staining (blue asterisks), and the areas of GFAP-positive cells (white dots) are also showing sparse TUNEL-positive cells (black dots).

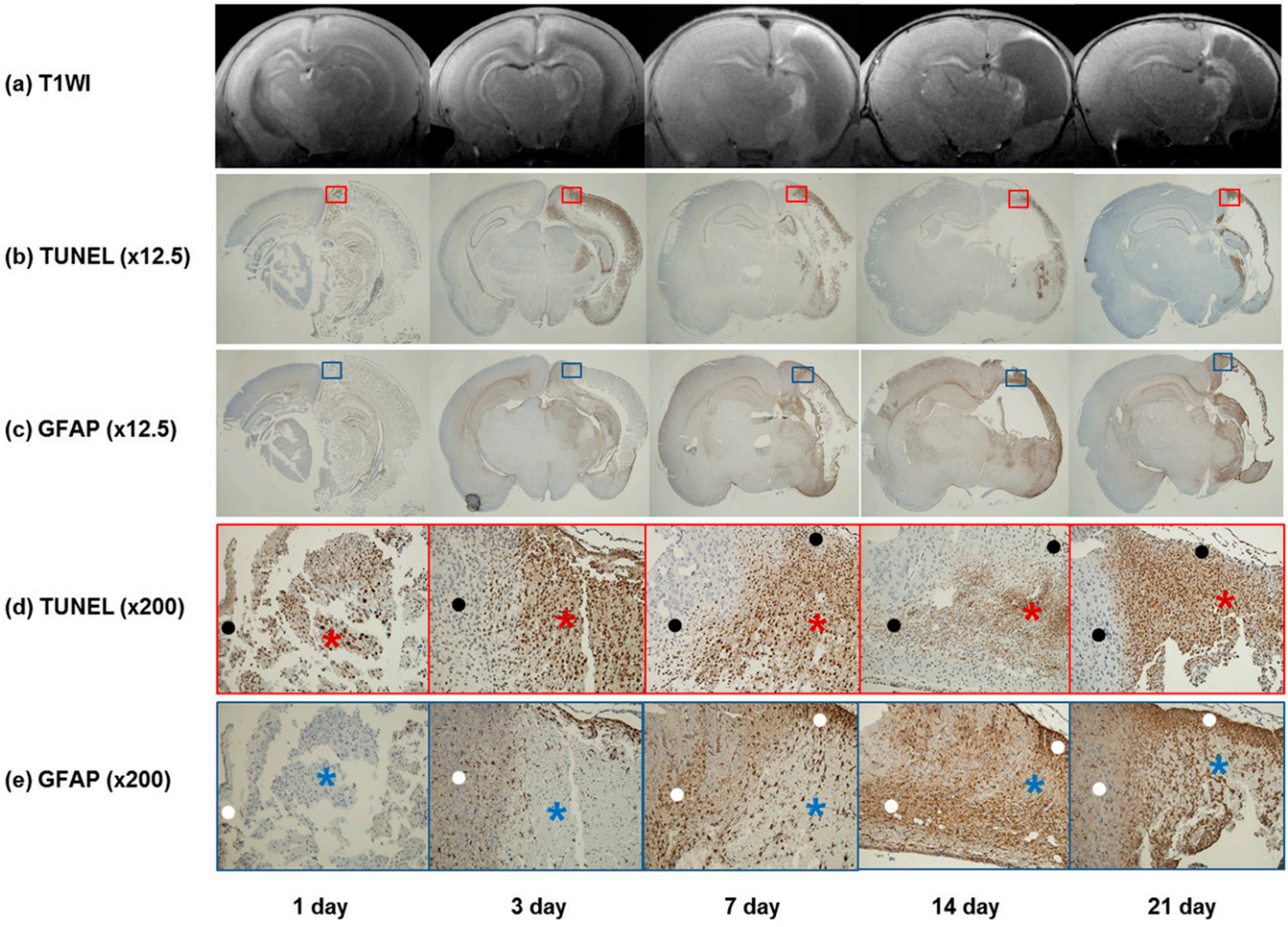

showed delayed HMON enhancement up to 21 days after HII and distribution of HMON enhancement on MR images was in good agreement with that of the TUNEL-positive cells, which is suggestive of apoptosis. In contrast, the distribution of GFAP staining did not correspond to that of HMON enhancement. These results suggest that apoptosis may be the dominant mechanism for HMON enhancement.

However, there was a lack of HMON enhancement at 1 day, although the histological abnormality existed. Plausible explanations for the lack of HMON enhancement at 1 day are temporal dysfunction of microtubules that are sensitive to ischaemic injury, low concentration of contrast in the serum by the intraperitoneal route and cytotoxic oedema.[10,12,15] In addition, the number of apoptotic cells in the injured hemisphere peaked at 3 days and decreased by 21 days. This change was not in agreement with the pattern of HMON enhancement, which showed an increase in the mean relative contrast value from 1 day to 21 days. This suggests that other factors, in addition to apoptosis, may also contribute to HMON enhancement. The pathophysiology of manganese enhancement in MR images has been previously discussed in relation to experimental animal models of hypoxia; manganese enhancement was closely related to activated microglia, reactive astrogliosis, calcium ion channel activity, blood–brain barrier disruption and apoptosis.[9,13–15,25] Although we did not precisely evaluate these potential factors such as activated microglia, calcium ion channel activity and blood–brain barrier disruption, they may have partially contributed to the HMON enhancement.

The ADC value derived from diffusion-weighted images can delineate ischaemic changes in the brain during an early

period.[10,11] In our study, ADC values tended to decrease quickly at 1 day following HII and then normalized after a period of time. Thus, ADC values do not reflect the ischaemic changes during the later period in spite of the presence of histologic changes. In our study, there was a signal loss in the injured dorsolateral thalamus on diffusion-weighted images and ADC maps. This can be explained by the phenomenon called "T_2 blackout",[26] which represents susceptibility effects caused by paramagnetic effects of HMON. In contrast with ADC measurement, HMON-enhanced MRI may have an advantage in visualizing apoptotic area even in the later period after ischaemic injury.

The limitations of our study are as follows. First, the mechanism of HMON accumulation in the apoptotic area remains unclear, although we inferred it. Second limitation of our study is that HMON was given by intraperitoneal injection, which is not commonly used in clinical practice. Further research is needed to apply HMON in practice. Third, HMON was administered prior to the onset of hypoxia and was administered only once. The clinical application of HMON might be limited by long duration of contrast action and consequential inability to separate the effects of T_1 relaxivity changes and enhancement.

In conclusion, the areas of HMON enhancement showed best spatial agreement with those of apoptosis on TUNEL staining. Both HMON enhancement and TUNEL-positive cells were observed up to 21 days after HII. The strength of our study is the visualization of apoptotic area *in vivo* using HMON-enhanced MRI, and we showed that HII has a prolonged evolution lasting for several weeks. For the development of neuroprotective agents, an imaging method that can depict and monitor apoptotic area after HII is necessary. This study demonstrated that HMON-enhanced MRI will provide a pivotal role in monitoring early results of therapeutic trials and in guiding the development of practical treatment strategies. The results of our study also suggest that therapeutic efforts to save the injured neurons can be adjusted up to 3 weeks following HII.

FUNDING

This study was supported by Samsung Biomedical Research Institute grant (grant no. C-A8-303-1).

REFERENCES

1. Ferriero DM. Neonatal brain injury. *N Engl J Med* 2004; **351**: 1985–95. doi: http://dx.doi.org/10.1056/NEJMra041996
2. Volpe JJ. Brain injury in premature infants: a complex amalgam of destructive and developmental disturbances. *Lancet Neurol* 2009; **8**: 110–24. doi: http://dx.doi.org/10.1016/S1474-4422(08)70294-1
3. Northington FJ, Ferriero DM, Graham EM, Traystman RJ, Martin LJ. Early neurodegeneration after hypoxia-ischemia in neonatal rat is necrosis while delayed neuronal death is apoptosis. *Neurobiol Dis* 2001; **8**: 207–19. doi: http://dx.doi.org/10.1006/nbdi.2000.0371
4. Geddes R, Vannucci RC, Vannucci SJ. Delayed cerebral atrophy following moderate hypoxia-ischemia in the immature rat. *Dev Neurosci* 2001; **23**: 180–5. doi: http://dx.doi.org/46140
5. Azzopardi DV, Strohm B, Edwards AD, Dyet L, Halliday HL, Juszczak E, et al. Moderate hypothermia to treat perinatal asphyxial encephalopathy. *N Engl J Med* 2009; **361**: 1349–58. doi: http://dx.doi.org/10.1056/NEJMoa0900854
6. Liao Y, Cotten M, Tan S, Kurtzberg J, Cairo MS. Rescuing the neonatal brain from hypoxic injury with autologous cord blood. *Bone Marrow Transplant* 2013; **48**: 890–900. doi: http://dx.doi.org/10.1038/bmt.2012.169
7. van Velthoven CT, Sheldon RA, Kavelaars A, Derugin N, Vexler ZS, Willemen HL, et al. Mesenchymal stem cell transplantation attenuates brain injury after neonatal stroke. *Stroke* 2013; **44**: 1426–32. doi: http://dx.doi.org/10.1161/STROKEAHA.111.000326
8. Gonzalez FF, Larpthaveesarp A, McQuillen P, Derugin N, Wendland M, Spadafora R, et al. Erythropoietin increases neurogenesis and oligodendrogliosis of subventricular zone precursor cells after neonatal stroke. *Stroke* 2013; **44**: 753–8. doi: http://dx.doi.org/10.1161/STROKEAHA.111.000104
9. Wideroe M, Brekken C, Kavelaars A, Pedersen TB, Goa PE, Heijnen C, et al. Longitudinal manganese-enhanced magnetic resonance imaging of delayed brain damage after hypoxic-ischemic injury in the neonatal rat. *Neonatology* 2011; **100**: 363–72. doi: http://dx.doi.org/10.1159/000328705
10. Yang J, Wu EX. Manganese-enhanced MRI detected the gray matter lesions in the late phase of mild hypoxic-ischemic injury in neonatal rat. *Conf Proc IEEE Eng Med Biol Soc* 2007; **2007**: 51–4. doi: http://dx.doi.org/10.1109/IEMBS.2007.4352220
11. Wang Y, Cheung PT, Shen GX, Wu EX, Cao G, Bart I, et al. Hypoxic-ischemic brain injury in the neonatal rat model: relationship between lesion size at early MR imaging and irreversible infarction. *AJNR Am J Neuroradiol* 2006; **27**: 51–4.
12. Xia XY, Ikeda T, Ota A, Xia YX, Sameshima H, Ikenoue T, et al. Heat shock protein 72 expression and microtubule-associated protein 2 disappearance after hypoxia-ischemia in the developing rat brain. *Am J Obstet Gynecol* 1999; **180**: 1254–62. doi: http://dx.doi.org/10.1016/S0002-9378(99)70625-3
13. Kawai Y, Aoki I, Umeda M, Higuchi T, Kershaw J, Higuchi M, et al. *In vivo* visualization of reactive gliosis using manganese-enhanced magnetic resonance imaging. *Neuroimage* 2010; **49**: 3122–31. doi: http://dx.doi.org/10.1016/j.neuroimage.2009.11.005
14. Haapanen A, Ramadan UA, Autti T, Joensuu R, Tyynela J. *In vivo* MRI reveals the dynamics of pathological changes in the brains of cathepsin D-deficient mice and correlates changes in manganese-enhanced MRI with microglial activation. *Magn Reson Imaging* 2007; **25**: 1024–31. doi: http://dx.doi.org/10.1016/j.mri.2007.03.012
15. Widerøe M, Olsen O, Pedersen TB, Goa PE, Kavelaars A, Heijnen C, et al. Manganese-enhanced magnetic resonance imaging of hypoxic-ischemic brain injury in the neonatal rat. *Neuroimage* 2009; **45**: 880–90.
16. Malecki EA. Manganese toxicity is associated with mitochondrial dysfunction and DNA fragmentation in rat primary striatal neurons. *Brain Res Bull* 2001; **55**: 225–8. doi: http://dx.doi.org/10.1016/S0361-9230(01)00456-7
17. Crossgrove J, Zheng W. Manganese toxicity upon overexposure. *NMR Biomed* 2004; **17**: 544–53. doi: http://dx.doi.org/10.1002/nbm.931
18. Shin J, Anisur RM, Ko MK, Im GH, Lee JH, Lee IS. Hollow manganese oxide nanoparticles as multifunctional agents for magnetic

resonance imaging and drug delivery. *Angew Chem Int Ed Engl* 2009; **48**: 321–4. doi: http://dx.doi.org/10.1002/anie.200802323

19. Ha TL, Kim HJ, Shin J, Im GH, Lee JW, Heo H, et al. Development of target-specific multimodality imaging agent by using hollow manganese oxide nanoparticles as a platform. *Chem Commun (Camb)* 2011; **47**: 9176–8. doi: http://dx.doi.org/10.1039/c1cc12961a
20. Rice JE 3rd, Vannucci RC, Brierley JB. The influence of immaturity on hypoxic-ischemic brain damage in the rat. *Ann Neurol* 1981; **9**: 131–41. doi: http://dx.doi.org/10.1002/ana.410090206
21. Vannucci RC, Vannucci SJ. Perinatal hypoxic-ischemic brain damage: evolution of an animal model. *Dev Neurosci* 2005; **27**: 81–6. doi: http://dx.doi.org/10.1159/000085978
22. Portera-Cailliau C, Price DL, Martin LJ. Excitotoxic neuronal death in the immature brain is an apoptosis-necrosis morphological continuum. *J Comp Neurol* 1997; **378**: 70–87.
23. Renolleau S, Aggoun-Zouaoui D, Ben-Ari Y, Charriaut-Marlangue C. A model of transient unilateral focal ischemia with reperfusion in the P7 neonatal rat: morphological changes indicative of apoptosis. *Stroke* 1998; **29**: 1454–60; discussion 1461. doi: http://dx.doi.org/10.1161/01.STR.29.7.1454
24. Li Y, Chopp M, Jiang N, Yao F, Zaloga C. Temporal profile of in situ DNA fragmentation after transient middle cerebral artery occlusion in the rat. *J Cereb Blood Flow Metab* 1995; **15**: 389–97. doi: http://dx.doi.org/10.1038/jcbfm.1995.49
25. Aoki I, Naruse S, Tanaka C. Manganese-enhanced magnetic resonance imaging (MEMRI) of brain activity and applications to early detection of brain ischemia. *NMR Biomed* 2004; **17**: 569–80. doi: http://dx.doi.org/10.1002/nbm.941
26. Hiwatashi A, Kinoshita T, Moritani T, Wang HZ, Shrier DA, Numaguchi Y, et al. Hypointensity on diffusion-weighted MRI of the brain related to T2 shortening and susceptibility effects. *AJR Am J Roentgenol* 2003; **181**: 1705–9. doi: http://dx.doi.org/10.2214/ajr.181.6.1811705